Journal of Cellular Biochemistry 102:98–109 (2007)

An ROS Generator, Antimycin A, Inhibits the Growth of HeLa Cells Via Apoptosis

Woo Hyun Park,*† Yong Whan Han, Suhn Hee Kim, and Sung Zoo Kim

Department of Physiology, Medical School, Institute for Medical Sciences, Centers for Healthcare Technology Development, Chonbuk National University, JeonJu, 561-180, Republic of Korea

Abstract Antimycin A (AMA), an inhibitor of electron transport in mitochondria, has been used as a reactive oxygen species (ROS) generator in biological systems. Here, we investigated the in vitro effect of AMA on apoptosis in HeLa cells. AMA inhibited the growth of HeLa cells with an IC_{50} of about 50 μM. AMA efficiently induced apoptosis, as evidenced by flow cytometric detection of sub-G1 DNA content, annexin V binding assay, and DAPI staining. This apoptotic process was accompanied by the loss of mitochondrial membrane potential ($\Delta\Psi_m$), Bcl-2 down-regulation, Bax up-regulation, and PARP degradation. All caspase inhibitors used in this experiment, especially pan-caspase inhibitor (Z-VAD), could rescue some HeLa cells from AMA-induced cell death. When we examined the changes of the ROS, H_2O_2 or $O_2^{\cdot-}$, in AMA-treated cells, H_2O_2 and $O_2^{\cdot-}$ were markedly increased. In addition, we detected the depletion of GSH content in AMA-treated cells. Pan-caspase inhibitor showing the efficient anti-apoptotic effect significantly reduced GSH depletion by AMA. Superoxide dismutase (SOD) and catalase did not reduce intracellular ROS, but these could strongly rescue the cells from apoptosis. However, these anti-apoptotic effects were not accompanied by the recovery of GSH depletion. Interestingly, catalase significantly decreased the CMF negative (GSH depletion) and propidium iodide (PI) positive cells, indicating that catalase strongly maintained the integrity of the cell membrane in CMF negative cells. Taken together, these results demonstrate that AMA potently generates ROS, induces the depletion of GSH content in HeLa cells, and strongly inhibits the growth of HeLa cells throughout apoptosis. J. Cell. Biochem. 102: 98–109, 2007.

Key words: Antimycin A; ROS; Apoptosis; HeLa; Caspase; Mitochondria; SOD; Catalase; GSH

Reactive oxygen species (ROS) include hydrogen peroxide (H_2O_2), nitric oxide (NO), superoxide anion ($O_2^{\cdot-}$), hydroxyl radical ($^{\cdot}OH$), and peroxynitrite ($ONOO^-$). These molecules have recently been implicated in the regulation of many important cellular events, including transcription factor activation, gene expression, differentiation, and cellular proliferation [Gonzalez et al., 2002; Baran et al., 2004; Bubici et al., 2006]. ROS are formed as byproducts of mitochondiral respiration or precise oxidases, including nicotine adenine diphosphate (NADPH) oxidase, xanthine oxidase (XO), and certain arachidonic acid oxygenases [Zorov et al., 2006]. A change in the redox state of the tissue implies a change in ROS generation or metabolism. Principal metabolic pathways include superoxide dismutase (SOD), which is expressed as extracellular, intracellular, and mitochondiral isoforms. These isoforms metabolize $O_2^{\cdot-}$ to H_2O_2. Further metabolism by peroxidases that include catalase and glutathione (GSH) peroxidase yields O_2 and H_2O [Wilcox, 2002]. Cells possess antioxidant systems to control the redox state, which is important for their survival. Excessive production of

Abbreviations used: AMA, antimycin A; ROS, reactive oxygen species; NADPH, nicotine adenine diphosphate; XO, xanthine oxidase; SOD, superoxide dismutase; PARP, poly(ADP-ribose) polymerase (PARP); FBS, fetal bovine serum; MTT, 3-(4,5-dimethylthiazol-2-yl)-2,5-diphenyltetrazolium bromide; PI, propidium iodide; PBS, phosphate buffer saline; FITC, fluorescein isothiocyanate; DAPI, 4′-6-Diamidino-2-phenylindoleH_2DCFDA, 2′,7′-Dichlorodihydrofluorescein diacetate; DHE, dihydroethidium; GSH, glutathione; CMFDA, 5-chloromethylfluorescein diacetate.

†Assistant Professor.

Grant sponsor: Korean Science and Engineering Foundation; Grant number: R01-2006-000-10544-0.

*Correspondence to: Woo Hyun Park, PhD, Department of Physiology, Medical School, Center for Healthcare Technology Development, Chonbuk National University, JeonJu, Republic of Korea. E-mail: parkwh71@chonbuk.ac.kr

Received 4 October 2006; Accepted 3 January 2007

DOI 10.1002/jcb.21280

ROS gives rise to the activation of events that lead to death or survival in several cell types [Simon et al., 2000; Chen et al., 2006; Dasmahapatra et al., 2006; Wallach-Dayan et al., 2006]. The exact mechanisms involved in cell death induced by ROS are unknown, and the protective effect mediated by some antioxidants remains controversial.

Antimycin A (AMA) is a product that is predominantly composed of antimycin A1 and A3 derived from *Streptomyces Kitazawensis* (Fig. 1A) [Nakayama et al., 1956]. AMA inhibits succinate oxidase and NADH oxidase, and also inhibits mitochondrial electron transport between cytochrome *b* and *c* [Alexandre and Lehninger, 1984; Campo et al., 1992; Maguire et al., 1992; Pham et al., 2000]. The inhibition of electron transport causes a collapse of the proton gradient across the mitochondrial inner membrane, thereby breaking down the mitochondrial membrane potential ($\Delta\Psi_m$) [Campo et al., 1992; Pham et al., 2000; Balaban et al., 2005]. This inhibition also causes the production of ROS [Panduri et al., 2004; Balaban et al., 2005]. There is evidence that either the presence of ROS or the collapse of mitochondrial membrane potential ($\Delta\Psi_m$) opens the mitochondrial permeability transition pore, which is accompanied by the release of proapoptotic molecules such as cytochrome *c* into the cytoplasm [Costantini et al., 1996; Pastorino et al., 1999; Petronilli et al., 2001]. Because AMA acts directly on the mitochondria, AMA-induced apoptosis has been reported in

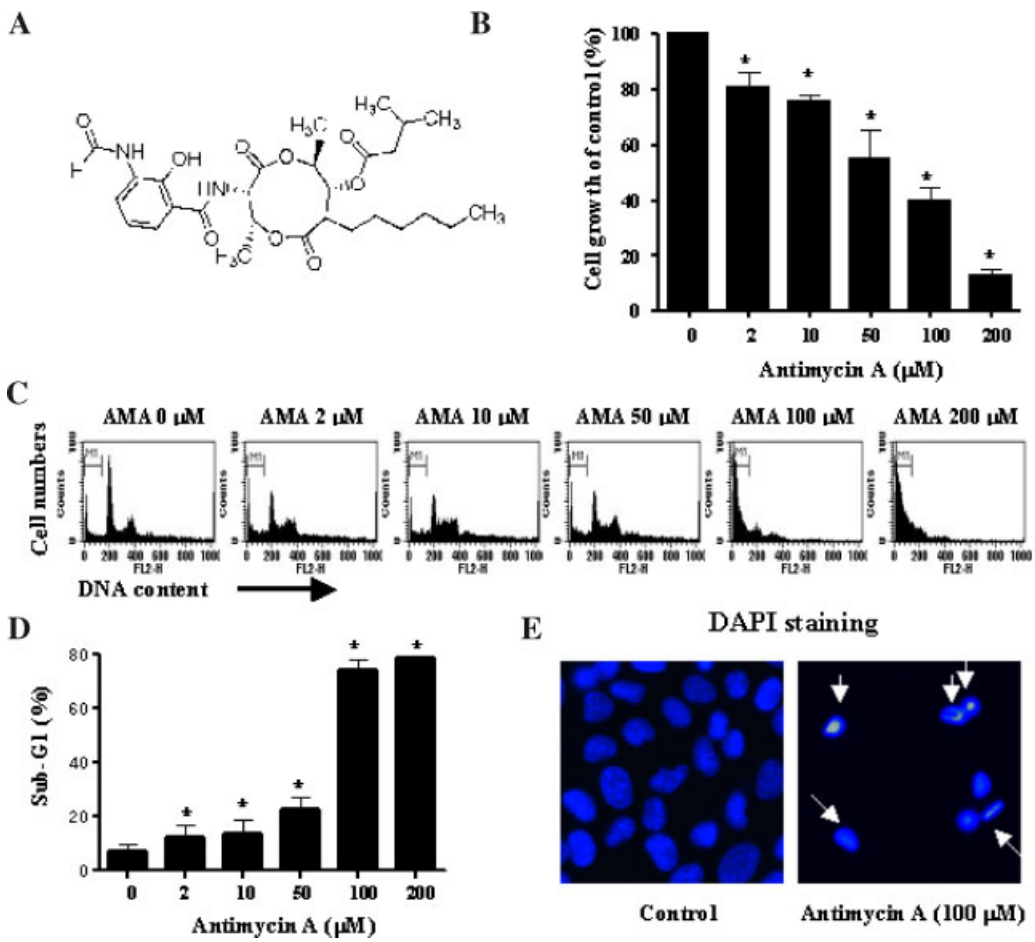

Fig. 1. Effects of AMA on the growth inhibition of HeLa cells in vitro. **A**: Structure of AMA. **B**: Exponentially growing cells were treated with the indicated concentrations of AMA for 72 h. Cell growth inhibition was assessed by MTT assays. **C**: Sub-G1 cells were measured with DNA flow cytometric analysis. **D**: The graph shows the sub-G1 percentage of (C). **E**: Cells were treated with or without AMA (100 μM) for 72 h, stained with DAPI, and observed under a fluorescence microscope (×400). The arrows indicate apoptotic nuclei with condensed chromatin. $^*P < 0.05$ compared with the AMA-untreated control group. [Color figure can be viewed in the online issue, which is available www.interscience.wiley.com.]

many experiments [Wolvetang et al., 1994; Kaushal et al., 1997; de Graaf et al., 2002; King, 2005].

In the present study, we evaluated the effects of AMA as a ROS generator on the growth of human cervical adenocarcinoma HeLa cells, and describe its mechanism.

MATERIALS AND METHODS

Cell Culture

Human cervical adenocarcinoma HeLa cells were maintained in humidified room air containing 5% CO_2 at 37ºC. HeLa cells were cultured in Dulbecco's modified Eagle's medium (DMEM) supplemented with 10% fetal bovine serum (FBS) and 1% penicillin-streptomycin (GIBCO BRL, Grand Island, NY). Cells were routinely grown in 100 mm plastic tissue culture dishes (Nunc, Roskilde, Denmark) and harvested with a solution of trypsin-EDTA when they were in logarithmic phase of growth. Cells were maintained at these culture conditions for all experiments.

Reagents

AMA was purchased from Sigma-Aldrich Chemical Company (St. Louis, MO). AMA was dissolved in ethanol at 2×10^{-2} M as a stock solution. Pan-caspase inhibitor (Z-VAD-FMK), caspase-3 inhibitor (Z-DEVD-FMK), caspase-8 inhibitor (Z-IETD-FMK), and caspase-9 inhibitor (Z-LEHD-FMK) were obtained from R&D Systems, Inc. (Minneapolis, MN) and dissolved in DMSO (Sigma). SOD and catalase were obtained from Sigma. These were dissolved in 50 mM potassium phosphate buffer at 4,733 U/ml. All of the stock solutions were wrapped in foil and kept at 4°C or −20°C.

Growth Inhibition Assay

The in vitro growth inhibition effect of AMA on HeLa cells was determined by measuring 3-(4,5-dimethylthiazol-2-yl)-2,5-diphenyltetrazolium bromide (MTT) dye absorbance of living cells as described previously [Park et al., 2000]. In brief, cells (2×10^5 cells per well) were seeded in 96-well microtiter plates (Nunc). After exposure to the drug for 72 h, 50 μl of MTT (Sigma) solution (2 mg/ml in PBS) were added to each well, and the plates were incubated for additional 3 or 4 h at 37°C. MTT solution in medium was aspirated off. To achieve solubilization of the formazan crystals formed in viable cells, 100 or 200 μl of DMSO were added to each well. The optical density of each well was measured at 570 nm using a microplate reader (Spectra MAX 340, Molecular Devices Co., Sunnyvale, CA). Each plate contained multiple wells at a given experimental condition and multiple control wells. This procedure was replicated for 2–4 plates/condition.

Sub-G1 Analysis

Sub-G1 distributions were determined by staining DNA with propidium iodide (PI; Sigma) as described previously [Park et al., 2000, 2003]. In brief, 1×10^6 cells were incubated with the designated doses of AMA, SOD, and catalase for 72 h. Cells were then washed in phosphate-buffered saline (PBS) and fixed in 70% ethanol. Cells were again washed with PBS and then incubated with PI (10 μg/ml) with simultaneous treatment of RNase at 37°C for 30 min. The percentages of cells containing sub-G1 DNA were measured with a FACStar flow cytometer (Becton Dickinson, San Jose, CA) and analyzed using lysis II and Cellfit software (Becton Dickinson).

Western Blot Analysis

Cells were incubated with the designated doses of AMA for 72 h. The cells were then washed in PBS and suspended in 5 volumes of lysis buffer (20 mM HEPES pH 7.9, 20% Glycerol, 200 mM KCl, 0.5 mM EDTA, 0.5% NP40, 0.5 mM DTT, 1% protease inhibitor cocktail (from Sigma)). The lysates were then collected and stored at −20°C until further use. The supernatant protein concentration was determined by the Bradford method. Supernatant samples containing 40 μg of total protein were resolved by a 8, 12.5, or 15% SDS–PAGE gel depending on the target protein sizes, transferred onto an Immobilon-P PVDF membrane (Millipore, MA) by electroblotting, and probed with anti-Bax, anti-Bcl-2, anti-caspase-3, and anti-PARP (Santa Cruz Biotechnology, Santa Cruz, CA). The membranes were incubated with horseradish peroxidase-conjugated secondary antibodies. The membrane blots were developed using an ECL kit (Amersham, Arlington Heights, IL).

Annexin V/PI Staining

Apoptosis was determined by staining cells with annexin V-fluorescein isothiocyanate (FITC) and PI labeling, because annexin V can

identify the externalization of phosphatidylserine during the progression of apoptosis and, therefore, can detect cells early in apoptosis. In brief, cells were incubated with the designated doses of AMA combined with or without caspase inhibitors, SOD, or catalase for 72 h. Cells were washed twice with cold PBS and then resuspended in 500 μl of binding buffer (10 mM HEPES/NaOH pH 7.4, 140 mM NaCl, 2.5 mM $CaCl_2$) at a concentration of 1×10^6 cells/ml. Five microliters of annexin V-FITC (PharMingen, San Diego, CA) and PI (1 μg/ml) were then added to these cells, which were analyzed with a FACStar flow cytometer (Becton Dickinson). Viable cells were negative for both PI and annexin V; apoptotic cells were positive for annexin V and negative for PI, whereas late apoptotic dead cells displayed both high annexin V and PI labeling. Non-viable cells, which underwent necrosis, were positive for PI and negative for annexin V.

Measurement of Mitochondrial Membrane Potential ($\Delta\psi_m$)

The mitochondrial membrane was monitored using the fluorescent dye Rhodamine 123, a cell permeable cationic dye, which preferentially enters mitochondria based on the highly negative mitochondrial membrane potential ($\Delta\psi_m$). Depolarization of mitochondrial membrane potential ($\Delta\psi_m$) results in the loss of Rhodamine 123 from the mitochondria and a decrease in intracellular fluorescence. In brief, cells were incubated with the designated doses of AMA combined with or without caspase inhibitors, SOD, or catalase for 72 h. Cells were washed twice with PBS and incubated with Rhodamine 123 (0.1 μg/ml; Sigma) at 37°C for 30 min. PI (1 μg/ml) was subsequently added, and Rhodamine 123 and PI staining intensity were determined by flow cytometry.

Morphological Analysis of Apoptosis by Staining With 4′-6-Diamidino-2-phenylindole (DAPI)

Cell morphology was evaluated by fluorescence microscopy following DAPI staining. The cells were cultured in eight-chamber glass slides (Lab-Tek, Nunc, Naperville, IL) containing 10% FBS in the absence or presence of AMA (100 μM). After 72 h of incubation, the slides were then rinsed with PBS and fixed in 80% ethanol for at least 30 min. Cellular DNA was stained with 1 μg/ml of DAPI dissolved in PBS for 30 min. The slides were then visualized on a Carl Zeiss fluorescence microscope (Germany). DAPI permeates the plasma membrane and yields blue chromatin. Viable cells display normal nuclear size and blue fluorescence, whereas apoptotic cells show condensed chromatin and fragmented nuclei.

Detection of Intracellular H_2O_2 and $O2^{\cdot-}$ Concentration

Intracellular H_2O_2 concentration was detected by means of an oxidation-sensitive fluorescent probe dye, 2′,7′-Dichlorodihydrofluorescein diacetate (H_2DCFDA) (Invitrogen Molecular Probes, Eugene, OR). H_2DCFDA was deacetylated intracellularly by non-specific esterase, which was further oxidized by cellular peroxides, yielding the fluorescent compound 2,7-dichlorofluorescein (DCF). Dihydroethidium (DHE) (Invitrogen Molecular Probes) is a fluorogenic probe that is highly selective for the detection of superoxide anion radicals. DHE is cell permeable and reacts with superoxide anion to form ethidium, which in turn intercalates in the deoxyribonucleic acid, thereby exhibiting a red fluorescence. In brief, cells were incubated with the designated doses of AMA combined with or without caspase inhibitors, SOD, or catalase for 72 h. Cells were then washed in PBS and incubated with 20 μM H_2DCFDA or 5 μM DHE at 37°C for 30 min according to the instructions of the manufacturer. DCF fluorescence and red fluorescence were detected by a FACStar flow cytometer (Becton Dickinson). For each sample, 5,000 or 10,000 events were collected. H_2O_2 and $O2^{\cdot-}$ production were expressed as mean fluorescence intensity (MFI), which was calculated by CellQuest software.

Detection of Intracellular Glutathione (GSH)

Cellular GSH levels were analyzed using 5-chloromethylfluorescein diacetate (CMFDA, Molecular Probes). CMFDA is a useful membrane-permeable dye for determining levels of intracellular GSH [Poot et al., 1991; Hedley and Chow, 1994; Macho et al., 1997]. In brief, cells were incubated with the designated doses of AMA combined with or without caspase inhibitors, SOD, or catalase for 72 h. Cells were then washed in PBS and incubated with 5 μM CMFDA at 37°C for 30 min according to the instructions of the manufacturer. Cytoplasmic esterases convert non-fluorescent CMFDA to fluorescent 5-chloromethylfluorescein, which

can then react with the GSH. CMF fluorescence intensity was determined by a FACStar flow cytometer (Becton Dickinson), which was calculated by CellQuest software. For each sample, 5,000 or 10,000 events were collected.

Statistical Analysis

Results represent the means of at least two or three independent experiments; bar, SEM. Statistical analysis was performed using Student's *t*-test to evaluate differences between the groups. Microsoft Excel software was used for this analysis. Statistical significance was defined as $P < 0.05$.

RESULTS

Effects of AMA on the Growth Inhibition in the HeLa Cell

We examined the effect of AMA on the growth of HeLa cells using an MTT assay. Dose-dependent inhibition of cell growth was observed in HeLa cells with an IC_{50} of approximately 50 μM following treatment with AMA for 72 h (Fig. 1B). We performed an in vitro apoptosis detection assay to determine whether AMA could induce apoptosis in HeLa cells. As shown in Figure 1C,D, AMA increased the sub-G1 population in a dose-dependent manner at 72 h. Following exposure to 100 μM AMA, the percentage of HeLa cells in the sub-G1 phase was elevated to about 70%. To characterize the cell death induced by AMA, we examined the nuclear morphologies of dying cells using a fluorescent DNA-binding agent, DAPI. HeLa cells treated with 100 μM of AMA at 72 h displayed typical morphological features of apoptosis cells, that is, condensed nuclei (Fig. 1E) with no cytoplasm stained with β-tubulin and separated apoptotic bodies (data not shown).

Effects of AMA on the Plasma Membrane, Mitochondrial Transmembrane Potential ($\Delta\Psi_m$), and Apoptotic-Related Proteins in HeLa Cells

To further confirm and evaluate the induction of apoptosis, we stained cells with annexin V and PI. As with the percentages of the sub-G1 group cells assessed by flow cytometry, the proportion of annexin V-staining cells in the AMA-treated cells was increased strongly in a dose-dependent manner (Fig. 2A,B), which supports the finding that AMA-induced HeLa

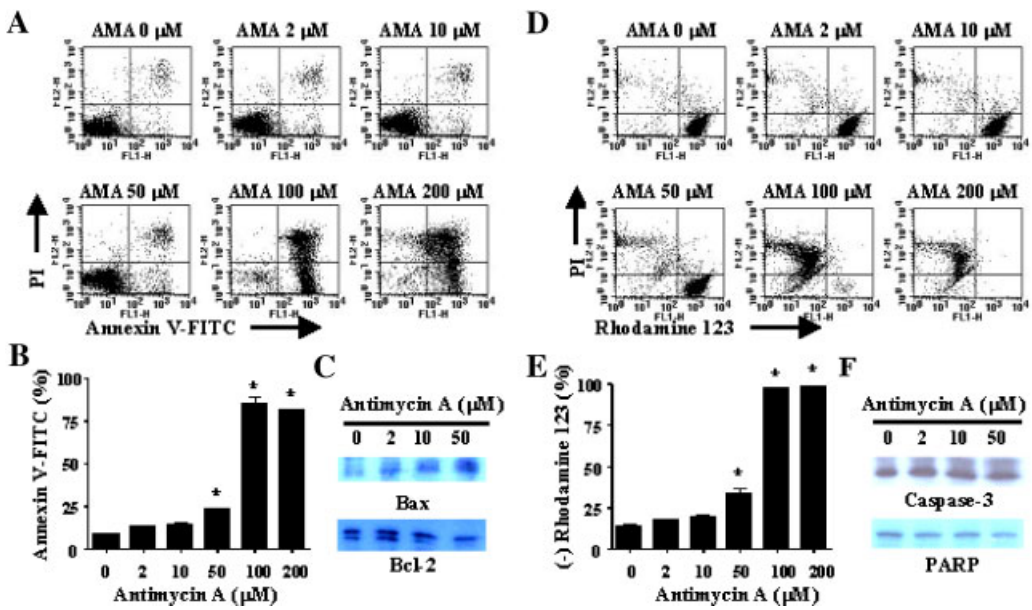

Fig. 2. Effects of AMA on the plasma membrane, mitochondrial transmembrane potential ($\Delta\Psi_m$), and apoptosis-related proteins in HeLa cells. Exponentially growing cells were treated with the indicated concentration of AMA for 72 h. **A**: Cells with annexin V staining were measured with a FACStar flow cytometer. **B**: The graph shows the percentages of annexin V positive cells from (A). **C**: Aliquots of 40 μg of protein extracts were resolved by 15% SDS–PAGE gel, transferred onto the PVDF membrane, and immunoblotted with the indicated antibodies, Bax and Bcl-2. **D**: Cells stained with Rhodamine 123 were measured with a FACStar flow cytometer. **E**: The graph shows the percentages of Rhodamine 123 negative cells from (D). **F**: Aliquots of 40 μg of protein extracts were resolved by 10–12.5% SDS–PAGE gel, transferred onto the PVDF membrane, and immunoblotted with the indicated antibodies, caspase-3 and PARP. $^*P < 0.05$ compared with the AMA-untreated control group. [Color figure can be viewed in the online issue, which is available www.interscience.wiley.com.]

cell death occurs via apoptosis. We also could detect HeLa cells with a modest amount of necrosis (annexin V negative and PI positive proportion cells).

Concerning the relationship between Bcl-2 and Bax regulation during AMA-induced apoptosis, Bcl-2 protein was decreased and Bax levels were increased at 72 h (Fig. 2C), which suggests that apoptosis induced by AMA may be mediated through the down- and up-regulation of apoptosis-related proteins in Bcl-2 and Bax in HeLa cells, respectively.

To elucidate the effect of AMA on mitochondrial membrane potential ($\Delta\Psi_m$), cells were treated with the indicated doses of AMA for 72 h. The percentages of cells staining negative for Rhodamine 123 showed a very similar pattern to the cells staining positive for annexin V after treatment with AMA (Fig. 2D,E). Following exposure to 100 μM AMA, the percentage of cells staining negative Rhodamine 123 was elevated to about 95%. Next, we wanted to determine whether AMA might activate caspase-3 during the induction of apoptosis, because caspase-3 plays an essential role as an executor in apoptosis. We observed that a 32 kDa precursor (procaspase-3) was very slightly degraded at the concentration of 50 μM AMA (Fig. 2F), indicating that the activation of caspase-3 was low. In regard to poly(ADP-ribose) polymerase (PARP) protein, a major substrate for executed caspases and a hallmark of apoptosis, Western blotting showed that the intact 116 kDa moiety of PARP was degraded by AMA (Fig. 2F). These results indicate conclusively that AMA-induced apoptosis in HeLa cells was accompanied by the loss of mitochondrial membrane potential ($\Delta\Psi_m$), Bcl-2 down-regulation, Bax up-regulation, and PARP degradation.

Effects of Caspase Inhibitors on AMA-Induced Apoptosis

To determine which caspases are required for the induction of apoptosis by AMA, we treated cells with pan-caspase inhibitor (Z-VAD-FMK), caspase-3 inhibitor (Z-DEVD-FMK), caspase-8 inhibitor (Z-IETD-FMK), and caspase-9 inhibitor (Z-LEHD-FMK) at a concentration of 12.5 μM (Fig. 3). Inhibitors for caspase-3, caspase-8, and caspase-9 did not prevent apoptotic events in AMA-treated HeLa cells at 72 h in view of annexin V positive staining (Fig. 3A,C), but decreased the loss of mitochondrial membrane potential ($\Delta\Psi_m$) (Fig. 3B,D). Pan-caspase inhibitor (Z-VAD-FMK) significantly reduced AMA-induced apoptosis (Fig. 3). When we used the caspase inhibitors at a dose of 25 μM, we did not observe any significant difference in the rescuing of cells from apoptosis (data not shown).

Effects of Caspase Inhibitors on ROS and GSH Production in AMA-Treated HeLa Cells

To elucidate the involvement of H_2O_2 in AMA-induced HeLa cell death, we assessed the H_2O_2 levels by using H_2DCFDA fluorescence. As shown in Fig. 4A,D, H_2O_2 levels were increased in HeLa cells exposed to AMA for 72 h. In regard to the H_2O_2 levels in relation to caspase inhibitors, inhibitors for caspase-3 and -8 significantly increased H_2O_2 levels in AMA-treated HeLa cells (Fig. 4A,D). However, pan-caspase inhibitor decreased the intracellular H_2O_2 levels (Fig. 4A,D). Next, we attempted to detect the change of $O_2^{\cdot-}$ in AMA-induced HeLa cell death. Red fluorescence derived from DHE, reflecting $O_2^{\cdot-}$ accumulation, was significantly increased in the AMA-treated cells (Fig. 4B,E). In regard to the $O_2^{\cdot-}$ levels in relation to caspase inhibitors, inhibitors for pan-caspase significantly reduced the intracellular $O_2^{\cdot-}$ levels (Fig. 4B,E). In contrast, inhibitor for caspase-8 significantly increased the intracellular $O_2^{\cdot-}$ levels (Fig. 4B,E).

Cellular GSH has been shown to be crucial for regulation of cell proliferation, cell cycle progression, and apoptosis [Poot et al., 1995; Schnelldorfer et al., 2000]. Therefore, we analyzed the changes of GSH levels of HeLa cells by using CMF fluorescence. The M1 population of HeLa cells showed a lower level of intracellular GSH content. AMA significantly elevated the percentages of cells residing in the M1 population, from 8% to 19% at 72 h (Fig. 4), indicating depletion of the intracellular GSH content of HeLa cells by AMA. Pan-caspase and caspase-3 inhibitors induced partial recovery of the GSH depletion induced by AMA. Inhibitors for caspase-8 and -9 did not alter the GSH content in AMA-treated cells (Fig. 4F).

Effects of SOD and Catalase on ROS Production, GSH Depletion, and Apoptosis in AMA-Treated HeLa Cells

Next, to determine whether ROS production and GSH depletion in AMA-treated HeLa cells were changed by SOD and catalase, HeLa cells

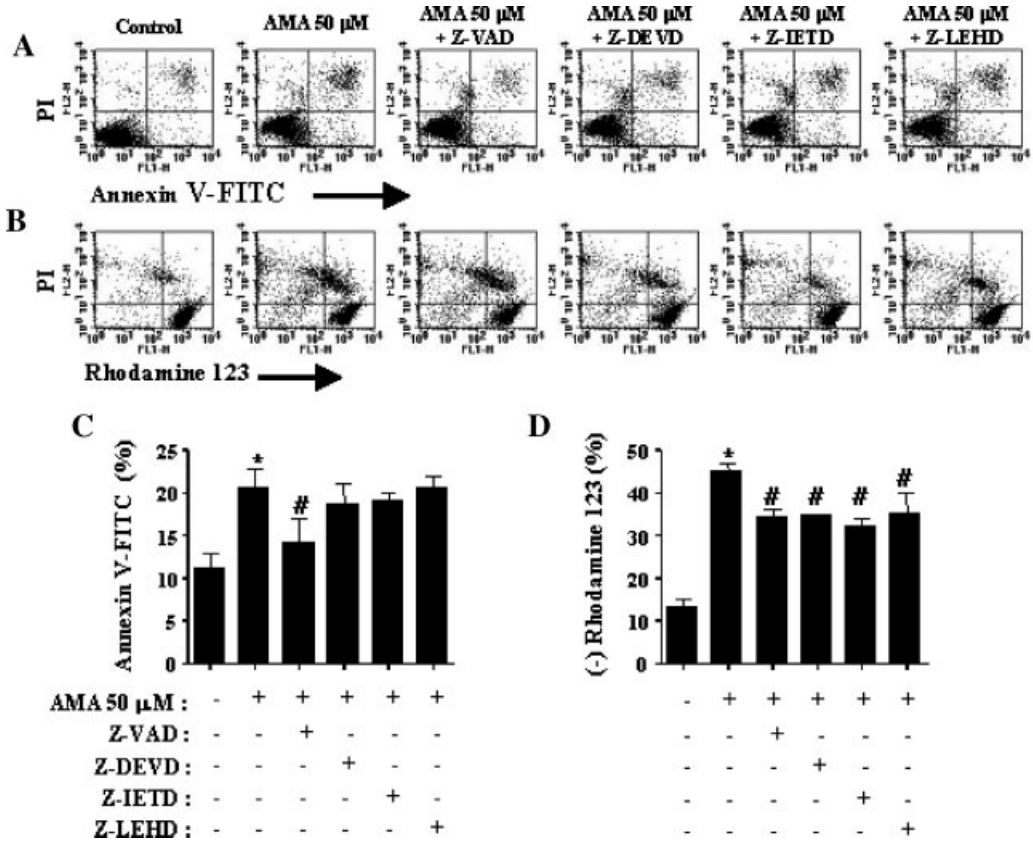

Fig. 3. Effects of caspase inhibitors on AMA-induced apoptosis. Exponentially growing cells were treated with the indicated caspase inhibitors (12.5 μM) in addition to AMA for 72 h. Annexin V staining cells (**A**) and Rhodamine 123 negative staining cells (**B**) were measured with a FACStar flow cytometer. The graphs show the percentage of annexin V positive staining cells from (A) (**C**) and Rhodamine 123 negative staining cells from (B) (**D**). $^{*}P < 0.05$ compared with the control group. $^{\#}P < 0.05$ compared with the cells treated with only AMA.

were treated with AMA in the presence or absence of SOD (30 U/ml) or/and catalase (30 U/ml) for 72 h. As shown in Figure 5A,D, SOD and catalase did not alter the level of H_2O_2 in AMA-treated HeLa cells. In regard to the $O_2^{\cdot-}$ levels in relation to SOD and catalase, neither changed the $O_2^{\cdot-}$ levels (Fig. 5B,E). When we assessed the levels of intracellular GSH, SOD and catalase could not inhibit the depletion of GSH content in HeLa cells treated with AMA (Fig. 5C,F), and no synergistic or additive effects of SOD and catalase on the ROS production and GSH content were detected.

Next, we examined whether SOD and catalase could prevent AMA-induced HeLa cell death. SOD and catalase significantly decreased apoptosis in HeLa cells treated with AMA (Fig. 6). Catalase strongly decreased apoptosis, by approximately 10%. In addition, catalase was stronger in reducing the loss of mitochondrial transmembrane potential ($\Delta\Psi_m$) in AMA-treated HeLa cells than SOD (22% vs. 9%) (Fig. 6C,F). There were no synergistic or additive effects of SOD and catalase on the reduction of apoptosis. In regard to CMF negative and PI positive cells, SOD did not reduce the proportion of CMF negative and PI positive cells induced by AMA. However, catalase significantly decreased the proportion of CMF negative and PI positive cells, indicating that catalase strongly maintained the integrity of the cell membrane in CMF negative cells (Fig. 7).

DISCUSSION

We focused on the apoptotic roles of AMA as a ROS generator in HeLa cells. We have also demonstrated that AMA inhibited the proliferation of HeLa cells by triggering apoptosis.

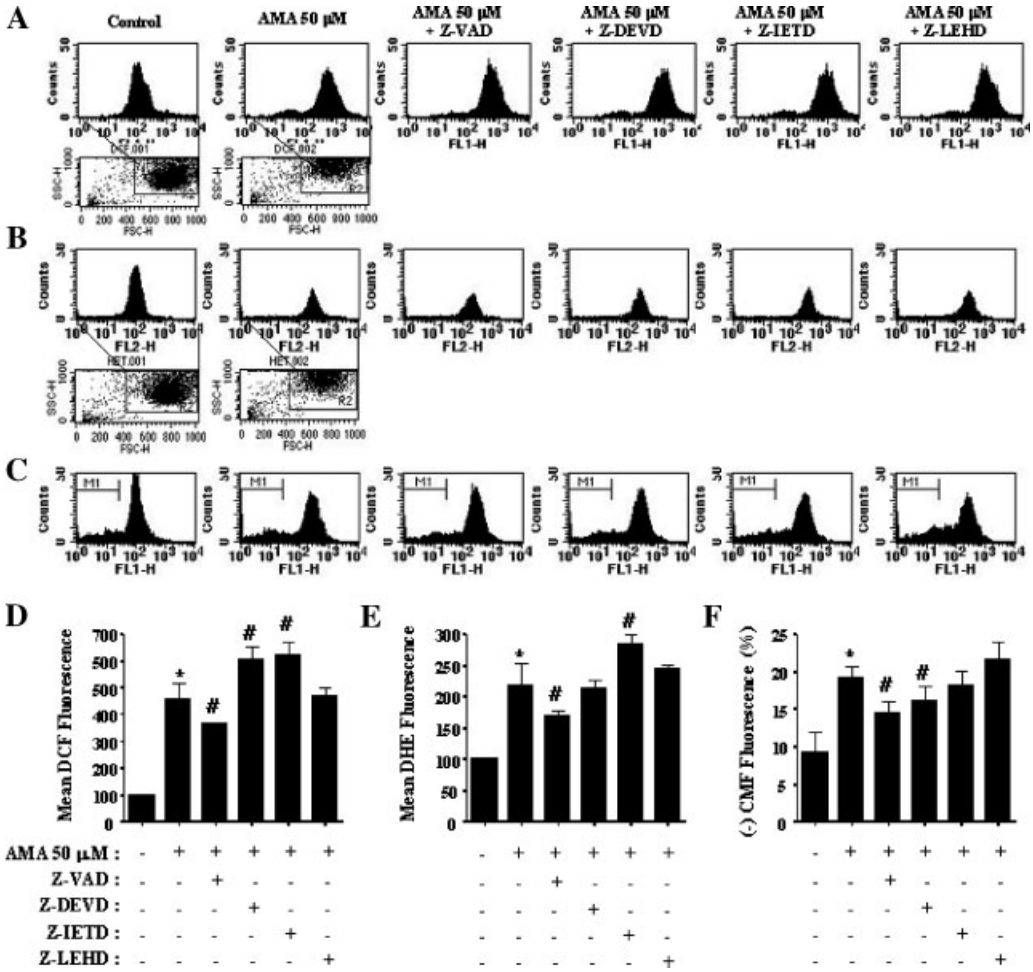

Fig. 4. Effects of caspase inhibitors on intracellular ROS and GSH production in AMA-treated HeLa cells. Exponentially growing cells were treated with the indicated caspase inhibitors (12.5 μM) in addition to AMA for 72 h. **A**: Intracellular H_2O_2 level, which is derived from the cells in the R2 region of the FSC and SSC dot plot. **B**: Intracellular O_2^- level from the R2 region. **C**: Intracellular GSH level. The graphs show the levels of mean DCF fluorescence of (A) (**D**), mean DHE fluorescence of (B) (**E**), and mean CMF fluorescence of (C) (**F**). $^*P < 0.05$ compared with the control group. $^{\#}P < 0.05$ compared with the cells treated with only AMA.

The susceptibility to AMA in assessment of apoptosis is dependent on cell type. For example, As4.1 juxtaglomerular cells were extremely sensitive, even to an AMA concentration of 50 nM concentration [Park et al., 2006]. However, this dose could not induce apoptosis in myelogenous leukemia HL-60 cells [King and Radicchi-Mastroianni, 2002; King, 2005] or in the HeLa cells used in this experiment and lung carcinoma Calu-6 cells (data not shown).

To gain insight into the molecular mechanism involved in apoptosis caused by AMA, expression of the apoptosis-related proteins and changes in mitochondrial transmembrane potential ($\Delta\Psi_m$) were assessed in HeLa cells. We predicted that the Bax to Bcl-2 ratio would be increased, since many apoptotic agents increase Bax protein and/or decrease Bcl-2 protein in their target cells during the apoptotic process. Similarly, we showed that induction of apoptosis was accompanied by elevation in the Bax to Bcl-2 ratio due to the up-regulation of Bax and down-regulation of Bcl-2 protein. p53 induces cell cycle arrest or apoptosis in response to DNA damage and regulates Bax and Bcl-2 protein expression [Coutts and La Thangue, 2006]. Unfortunately, in our experiment, we could not detect the basal expression of p53 protein in HeLa cells. However, we have reported that the expression of p53 was dramatically increased in AMA-treated As4.1 cells, suggesting that apoptosis is triggered by AMA

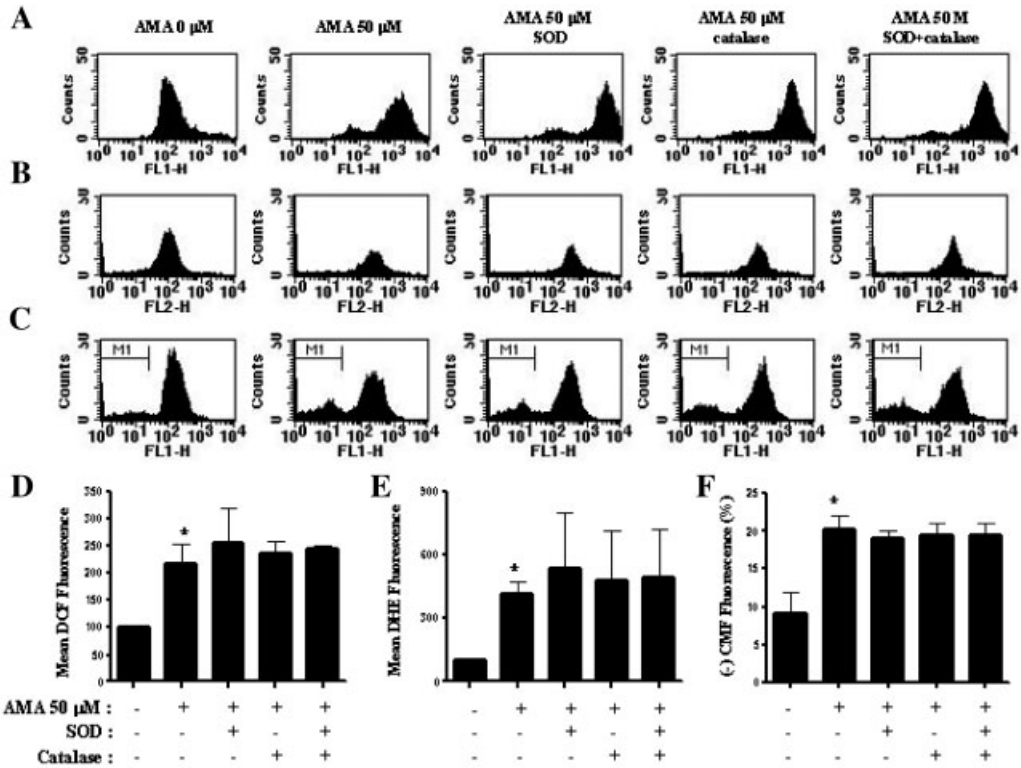

Fig. 5. Effects of SOD and catalase on the intracellular ROS and GSH production in AMA-treated HeLa cells. Exponentially-growing cells were treated with SOD and catalase in addition to AMA for 72 h. (**A**) The intracellular H_2O_2 levels. (**B**) The intracellular $O_2^{\cdot -}$ levels. (**C**) The intracellular GSH levels. The graphs show the levels of mean DCF fluorescence of A (**D**) and mean DHE fluorescence of B (**E**), and the percent of CMF negative fluorescence cells of C (**F**). * $P < 0.05$ as compared with the control group.

in a p53-dependent manner. Therefore, we could not rule out the role of p53 in apoptosis of HeLa cells induced by AMA. It has been suggested that a high ratio of Bax to Bcl-2 can cause the collapse of mitochondrial membrane potential ($\Delta\Psi_m$), resulting in the release of cytochrome *c* and apoptosis [Yang et al., 1997]. According to our data, AMA induced the loss of mitochondrial membrane potential ($\Delta\Psi_m$) in HeLa cells. Notably, there were similar levels of annexin V positive staining and Rhodamine 123 negative staining cells, which suggest that apoptosis is tightly connected to or dependent on the loss of mitochondrial membrane potential ($\Delta\Psi_m$).

Cytochrome *c* in cytosol forms an apoptosome that is composed of Aaf-1 and procaspase-9, resulting in activation of caspase-9. Caspase-9 activates the effector procaspases, including procaspase-3, to carry out the process of apoptosis [Cohen, 1997]. Correspondingly, caspase-3 was slightly activated and PARP protein was degraded by AMA in our experiments. To determine which caspases are required for the induction of apoptosis by AMA, we treated cells with caspase inhibitors. Only pan-caspase inhibitor (Z-VAD-FMK) significantly prevented the AMA-induced apoptosis for 72 h. However, caspase inhibitors for caspase-3, -8, and -9 slightly attenuated AMA-induced cell death, and activation of caspase-3 by antimycin was not significant. These data suggest that executor caspases such as caspase-6 and/or caspase-7 are required in addition to AMA for full induction of apoptosis. The modes of caspase activation during apoptosis by AMA may be dependent on cell type. Although there were differences in the incubation time and concentration of caspase inhibitors, inhibitors for pan-caspase and caspase-8 were effective for rescuing HL-60 cells from AMA-induced apoptosis [King and Radicchi-Mastroianni, 2002; King, 2005], and inhibitors for pan-caspase and caspase-8 could efficiently prevent the loss of mitochondrial membrane potential ($\Delta\Psi_m$) in AMA-treated As4.1 cells. Z-VAD could efficiently prevent the AMA-induced apoptosis in Calu-6 lung carcinoma cells, and inhibitors of

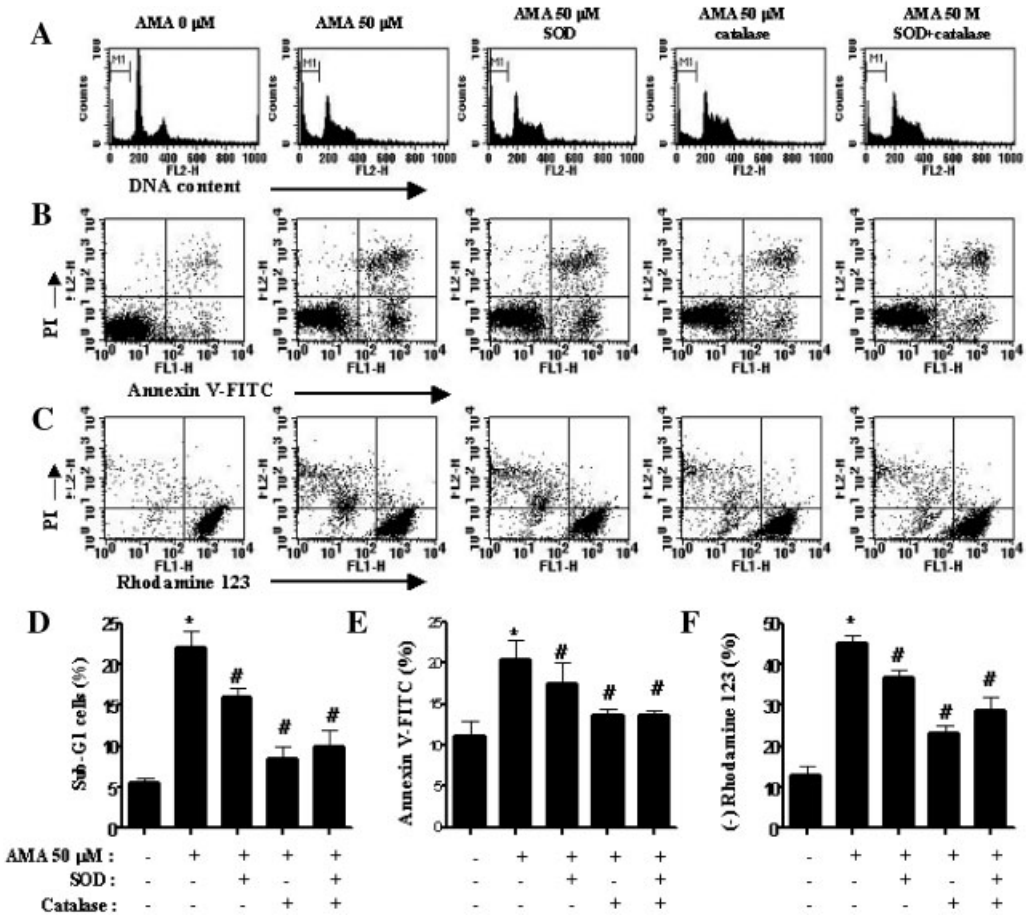

Fig. 6. Effects of SOD and catalase on AMA-induced apoptosis. Exponentially-growing cells were treated with SOD, catalase, and AMA for 72 h. (**A**) Sub-G1 cells, (**B**) annexin positive cells, and (**C**) Rhodamine 123 negative cells were measured by flow cytometric analysis as described in Materials and Methods. The graphs show the percentages of sub-G_1 population from (A) (**D**), annexin positive cells from (B) (**E**), and Rhodamine 123 negative cells from (C) (**F**). $^*P < 0.05$ compared with the control group. $^{\#}P < 0.05$ compared with the cells treated with only AMA.

caspase-3, -8, and -9 also performed weakly in these cells (unpublished data).

AMA can disturb the natural oxidation/reduction equilibrium in cells by causing a breakdown in the mitochondrial membrane potential ($\Delta\Psi_m$) [Campo et al., 1992; Pham et al., 2000; Balaban et al., 2005]. It has been reported that increased intracellular H_2O_2 plays an important role in AMA-induced cell death in liver cells [Chen et al., 2005; Chen and Yan, 2005] and A549 human lung cancer cells [Panduri et al., 2004]. Additionally, increases in $O_2^{\cdot-}$ levels by AMA were reported in human lung epithelial cells [Li et al., 2002]. These data suggest that the apoptotic effects of AMA are comparable to intracellular ROS levels, especially those of H_2O_2. Therefore, to elucidate the involvement of ROS such as H_2O_2 and $O_2^{\cdot-}$ in AMA-induced HeLa cell death, we assessed these ROS levels by using H_2DCFDA and DHE fluorescence. Our data showed that the intracellular H_2O_2 and $O_2^{\cdot-}$ levels were increased in the AMA-treated HeLa cells. Pan-caspase inhibitor, which reduced apoptosis induced by AMA, decreased the intracellular H_2O_2 and $O_2^{\cdot-}$ levels. However, caspase-8 inhibitor showing additional accumulation of H_2O_2 and $O_2^{\cdot-}$ did not enhance apoptosis, and the increase of H_2O_2 by caspase-3 inhibitor did not affect apoptosis in AMA-treated HeLa cells. In addition, SOD and catalase significantly inhibited apoptosis in AMA-treated HeLa cells without significant reduction of intracellular ROS levels. Our results indicated that the changes of ROS by AMA were not entirely correlated with apoptosis in HeLa cells. However, we cannot rule out

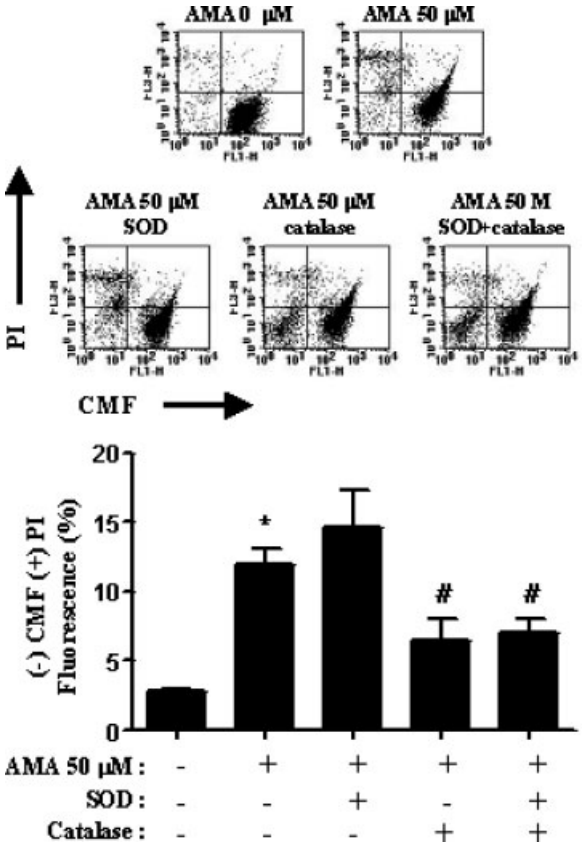

Fig. 7. Effects of SOD and catalase on CMF and PI fluorescence in AMA-treated HeLa cells. Exponentially growing cells were treated with the SOD and catalase in addition to AMA for 72 h. CMF fluorescence cells and PI positive staining cells were measured with a FACStar flow cytometer. The graph shows the percentages of CMF negative and PI positive staining cells from the above figures. $^{*}P < 0.05$ compared with the control group. $^{\#}P < 0.05$ compared with the cells treated with only AMA.

the possibility that the increased ROS levels by AMA influence only the cells at the early time to trigger apoptosis, because all the cells treated with agents were assessed at the time of 72 h in this experiment and we could detect the increased ROS levels within 20 min (data not shown). The exact mechanisms of cell death through intracellular ROS in AMA-treated HeLa cells still need to be defined further.

GSH is a main non-protein antioxidant in the cell, and it is able to clear away superoxide anion free radicals and provide electrons for enzymes such as GSH peroxidase, which reduces H_2O_2 to H_2O. It has been reported that the intracellular GSH content has a decisive effect on anticancer drug-induced apoptosis, indicating that apoptotic effects are inversely comparative to GSH content [Higuchi, 2004; Estrela et al., 2006]. Likewise, our results clearly indicated the depletion of intracellular GSH content by AMA in HeLa cells. In fact, pan-caspase inhibitor showing the inhibition of apoptosis in AMA-treated HeLa cells showed significant recovery of GSH depletion. However, SOD and catalase can rescue cells from AMA-induced cell death without recovery of GSH depletion. Catalase had a strong anti-apoptotic ability compared to SOD. This ability was supported by the observation that the cleavage of poly(ADP-ribose) polymerase (PARP) protein, a hallmark of apoptosis, was completely prevented by catalase in AMA-treated cells (data not shown). Interestingly, catalase strongly maintained the integrity of the plasma membrane in CMF negative cells (Fig. 7). These results suggest that GSH content depletion is not entirely, but is at least partially, correlated to apoptosis in HeLa cells, and also suggest that unknown catalase-regulated factors play a role in maintenance of plasma membrane integrity.

In conclusion, we have demonstrated that AMA potently generates ROS, induces the depletion of GSH content in HeLa cells, and potently inhibits the growth of HeLa cells through apoptosis.

ACKNOWLEDGMENTS

This research was supported by the Korean Science and Engineering Foundation (R01-2006-000-10544-0) and Korea Research Foundation Grant funded by the Government of the Republic of Korea (MOEHRD).

REFERENCES

Alexandre A, Lehninger AL. 1984. Bypasses of the antimycin a block of mitochondrial electron transport in relation to ubisemiquinone function. Biochim Biophys Acta 767:120–129.

Balaban RS, Nemoto S, Finkel T. 2005. Mitochondria, oxidants, and aging. Cell 120:483–495.

Baran CP, Zeigler MM, Tridandapani S, Marsh CB. 2004. The role of ROS and RNS in regulating life and death of blood monocytes. Curr Pharm Des 10:855–866.

Bubici C, Papa S, Pham CG, Zazzeroni F, Franzoso G. 2006. The NF-kappaB-mediated control of ROS and JNK signaling. Histol Histopathol 21:69–80.

Campo ML, Kinnally KW, Tedeschi H. 1992. The effect of antimycin A on mouse liver inner mitochondrial membrane channel activity. J Biol Chem 267:8123–8127.

Chen HM, Ma HH, Yan XJ. 2005. Inhibitory effect of agarohexaose on antimycin A induced generation of reactive oxygen species. Yao Xue Xue Bao 40:903–907.

Chen HM, Yan XJ. 2005. Antioxidant activities of agaro-oligosaccharides with different degrees of polymerization

in cell-based system. Biochim Biophys Acta 1722:103–111.
Chen TJ, Jeng JY, Lin CW, Wu CY, Chen YC. 2006. Quercetin inhibition of ROS-dependent and -independent apoptosis in rat glioma C6 cells. Toxicology 223: 113–126.
Cohen GM. 1997. Caspases: The executioners of apoptosis. Biochem J 326(Pt 1):1–16.
Costantini P, Chernyak BV, Petronilli V, Bernardi P. 1996. Modulation of the mitochondrial permeability transition pore by pyridine nucleotides and dithiol oxidation at two separate sites. J Biol Chem 271:6746–6751.
Coutts AS, La Thangue N. 2006. The p53 response during DNA damage: Impact of transcriptional cofactors. Biochem Soc Symp 73:181–189.
Dasmahapatra G, Rahmani M, Dent P, Grant S. 2006. The tyrphostin adaphostin interacts synergistically with proteasome inhibitors to induce apoptosis in human leukemia cells through a reactive oxygen species (ROS)-dependent mechanism. Blood 107:232–240.
de Graaf AO, Meijerink JP, van den Heuvel LP, DeAbreu RA, de Witte T, Jansen JH, Smeitink JA. 2002. Bcl-2 protects against apoptosis induced by antimycin A and bongkrekic acid without restoring cellular ATP levels. Biochim Biophys Acta 1554:57–65.
Estrela JM, Ortega A, Obrador E. 2006. Glutathione in cancer biology and therapy. Crit Rev Clin Lab Sci 43: 143–181.
Gonzalez C, Sanz-Alfayate G, Agapito MT, Gomez-Nino A, Rocher A, Obeso A. 2002. Significance of ROS in oxygen sensing in cell systems with sensitivity to physiological hypoxia. Respir Physiol Neurobiol 132: 17–41.
Hedley DW, Chow S. 1994. Evaluation of methods for measuring cellular glutathione content using flow cytometry. Cytometry 15:349–358.
Higuchi Y. 2004. Glutathione depletion-induced chromosomal DNA fragmentation associated with apoptosis and necrosis. J Cell Mol Med 8:455–464.
Kaushal GP, Ueda N, Shah SV. 1997. Role of caspases (ICE/CED 3 proteases) in DNA damage and cell death in response to a mitochondrial inhibitor, antimycin A. Kidney Int 52:438–445.
King MA. 2005. Antimycin A-induced killing of HL-60 cells: Apoptosis initiated from within mitochondria does not necessarily proceed via caspase 9. Cytometry A 63:69–76.
King MA, Radicchi-Mastroianni MA. 2002. Antimycin A-induced apoptosis of HL-60 cells. Cytometry 49:106–112.
Li C, Wright MM, Jackson RM. 2002. Reactive species mediated injury of human lung epithelial cells after hypoxia-reoxygenation. Exp Lung Res 28:373–389.
Macho A, Hirsch T, Marzo I, Marchetti P, Dallaporta B, Susin SA, Zamzami N, Kroemer G. 1997. Glutathione depletion is an early and calcium elevation is a late event of thymocyte apoptosis. J Immunol 158:4612–4619.
Maguire JJ, Kagan VE, Packer L. 1992. Electron transport between cytochrome c and alpha tocopherol. Biochem Biophys Res Commun 188:190–197.
Nakayama K, Okamoto F, Harada Y. 1956. Antimycin A: Isolation from a new Streptomyces and activity against rice plant blast fungi. J Antibiot (Tokyo) 9:63–66.
Panduri V, Weitzman SA, Chandel NS, Kamp DW. 2004. Mitochondrial-derived free radicals mediate asbestos-induced alveolar epithelial cell apoptosis. Am J Physiol Lung Cell Mol Physiol 286:L1220–L1227.
Park WH, Han YW, Kim SW, Kim SH, Cho KW, Kim SZ. 2006. Antimycin A induces apoptosis in As4.1 juxtaglomerular cells. Cancer Lett
Park WH, Jung CW, Park JO, Kim K, Kim WS, Im YH, Lee MH, Kang WK, Park K. 2003. Trichostatin inhibits the growth of ACHN renal cell carcinoma cells via cell cycle arrest in association with p27, or apoptosis. Int J Oncol 22:1129–1134.
Park WH, Seol JG, Kim ES, Hyun JM, Jung CW, Lee CC, Kim BK, Lee YY. 2000. Arsenic trioxide-mediated growth inhibition in MC/CAR myeloma cells via cell cycle arrest in association with induction of cyclin-dependent kinase inhibitor, p21, and apoptosis. Cancer Res 60:3065–3071.
Pastorino JG, Tafani M, Rothman RJ, Marcinkeviciute A, Hoek JB, Farber JL. 1999. Functional consequences of the sustained or transient activation by Bax of the mitochondrial permeability transition pore. J Biol Chem 274:31734–31739.
Petronilli V, Penzo D, Scorrano L, Bernardi P, Di Lisa F. 2001. The mitochondrial permeability transition, release of cytochrome c and cell death. Correlation with the duration of pore openings in situ. J Biol Chem 276: 12030–12034.
Pham NA, Robinson BH, Hedley DW. 2000. Simultaneous detection of mitochondrial respiratory chain activity and reactive oxygen in digitonin-permeabilized cells using flow cytometry. Cytometry 41:245–251.
Poot M, Kavanagh TJ, Kang HC, Haugland RP, Rabinovitch PS. 1991. Flow cytometric analysis of cell cycle-dependent changes in cell thiol level by combining a new laser dye with Hoechst 33342. Cytometry 12:184–187.
Poot M, Teubert H, Rabinovitch PS, Kavanagh TJ. 1995. De novo synthesis of glutathione is required for both entry into and progression through the cell cycle. J Cell Physiol 163:555–560.
Schnelldorfer T, Gansauge S, Gansauge F, Schlosser S, Beger HG, Nussler AK. 2000. Glutathione depletion causes cell growth inhibition and enhanced apoptosis in pancreatic cancer cells. Cancer 89:1440–1447.
Simon HU, Haj-Yehia A, Levi-Schaffer F. 2000. Role of reactive oxygen species (ROS) in apoptosis induction. Apoptosis 5:415–418.
Wallach-Dayan SB, Izbicki G, Cohen PY, Gerstl-Golan R, Fine A, Breuer R. 2006. Bleomycin initiates apoptosis of lung epithelial cells by ROS but not by Fas/FasL pathway. Am J Physiol Lung Cell Mol Physiol 290:L790–L796.
Wilcox CS. 2002. Reactive oxygen species: Roles in blood pressure and kidney function. Curr Hypertens Rep 4:160–166.
Wolvetang EJ, Johnson KL, Krauer K, Ralph SJ, Linnane AW. 1994. Mitochondrial respiratory chain inhibitors induce apoptosis. FEBS Lett 339:40–44.
Yang J, Liu X, Bhalla K, Kim CN, Ibrado AM, Cai J, Peng TI, Jones DP, Wang X. 1997. Prevention of apoptosis by Bcl-2: Release of cytochrome c from mitochondria blocked. Science 275:1129–1132.
Zorov DB, Juhaszova M, Sollott SJ. 2006. Mitochondrial ROS-induced ROS release: An update and review. Biochim Biophys Acta 1757:509–517.